Formin-mediated actin polymerization cooperates with Mud/Dynein during Frizzled/Dishevelled spindle orientation

Christopher A. Johnston[1,2,3,4,*], Laurina Manning[1,3], Michelle S. Lu[2], Ognjen Golub[2], Chris Q. Doe[1,2,3], and Kenneth E. Prehoda[2,*]

[1]Institute of Neuroscience, University of Oregon, Eugene, OR, 97403
[2]Institute of Molecular Biology and Department of Chemistry, University of Oregon, Eugene, OR, 97403
[3]Howard Hughes Medical Institute, University of Oregon, Eugene, OR, 97403
[4]Present address: Department of Biology, University of New Mexico, Albuquerque, NM, 87131
[*]Address for correspondence: Email: johnstca@unm.edu; Email: prehoda@uoregon.edu

JCS Advance Online Article. Posted on 18 July 2013

SUMMARY

To position the mitotic spindle, cytoskeletal components must be coordinated to generate cortical forces on astral microtubules. While the Dynein motor is common to many spindle orientation systems, 'accessory pathways' are often also required. In this work, we identify an accessory spindle orientation pathway that functions with Dynein during planar cell polarity, downstream of the Frizzled (Fz) effector Dishevelled (Dsh). Dsh contains a PDZ ligand and a Dynein-recruiting DEP domain that are both required for spindle orientation. The Dsh PDZ ligand recruits Canoe/Afadin and ultimately leads to Rho GTPase signaling mediated through RhoGEF2. The formin Diaphanous (Dia) functions as the Rho effector in this pathway, inducing F-actin enrichment at sites of cortical Dsh. Remarkably, chimeric protein experiments show that the Dia/actin accessory pathway can be replaced by an independent kinesin (Khc73) accessory pathway for Dsh-mediated spindle orientation. Our results define two "modular" spindle orientation pathways and show an essential role for actin regulation in Dsh-mediated spindle orientation.

INTRODUCTION

Oriented cell division is essential for the construction of complex tissue architecture during plant and animal development. For example, spindle alignment in epithelia ensures that daughter cells remain in the proper plane. Spindle positioning is also critical for asymmetric cell division, in which polarized fate determinants are segregated into one of two daughter cells. The position of the spindle can be regulated by interactions between the cell cortex and astral microtubules in which cortical polarity complexes provide directional cues for cytoskeletal filaments and motor proteins (Siller and Doe, 2009). The minus end directed motor dynein is a critical force-generating component in spindle orientation from yeast to mammals. However, robust spindle positioning can require that cortical signaling complexes initiate pathways that act synergistically with dynein (Johnston et al., 2009; Siegrist and Doe, 2005).

The Frizzled/Dishevelled (Fz/Dsh) planar cell polarity (PCP) pathway regulates oriented cell division in a broad range of animal cells (Morin and Bellaiche, 2011). For example, Fz/Dsh-mediated spindle orientation functions during the development of *Drosophila* bristle mechanosensory organs, in which posteriorly polarized Fz/Dsh determines anterior-posterior (A-P) orientation of the pI cell asymmetric division (Gho and Schweisguth, 1998). The Fz/Dsh complex also regulates spindle positioning in *C. elegans* blastomere development and zebrafish gastrulation (Segalen et al., 2010; Walston et al., 2004), highlighting an essential role of Fz/Dsh signaling for spindle orientation throughout evolution. The first downstream effector in Dsh-mediated spindle orientation was only recently identified: the adapter protein Mud interacts with the Dsh DEP domain and initiates a dynein-dependent connection to spindle microtubules (Segalen et al., 2010).

Here, we sought to identify additional Dsh-mediated pathways involved in spindle orientation that may function with Mud/Dynein. In certain contexts, Mud/Dynein requires additional pathways to achieve proper spindle alignment with cortical polarity. For example, in *Drosophila* neuroblasts the tumor suppressor Discs large (Dlg) binds the kinesin Khc73, and Dlg/Khc73 functions with Mud/Dynein for precise spindle orientation.

The protein Partner of Inscuteable (Pins) is polarized to the neuroblast apical cortex where it recruits both Mud and Dlg (Bowman et al., 2006; Siegrist and Doe, 2005; Siller et al., 2006). The cooperativity between these two pathways has been reconstituted in cultured S2 cells using an 'induced polarity' system in which the spindle aligns to artificially polarized Pins (Johnston et al., 2009). Although, the nature of the interplay between the Mud/Dynein and Dlg/Khc73 pathways is still being elucidated, the observation that Mud/Dynein does not function on its own in Pins-mediated spindle orientation prompted us to examine whether Fz/Dsh also requires an "accessory pathway" such as Dlg/Khc73.

RESULTS

To identify effectors that mediate spindle orientation downstream of Dsh (Fig. 1a), we used an 'induced polarity' spindle orientation assay in *Drosophila* S2 cells (Johnston et al., 2009). In this system, Dsh is fused to the COOH-terminus of the adhesion protein Echinoid (Ed), which forms polarized contacts in small cell clusters. Activity is then measured as spindle orientation relative to these Ed:Dsh induced cortical crescents (Fig. 1b). We found that the mitotic spindle aligns to crescents of Ed fused to the Dsh DEP domain plus adjacent C-terminus (Segalen et al., 2010) (Ed:DEP-CT; Fig. 1a,c). Although the DEP domain has been shown to function upstream of Mud/Dynein spindle orientation complex (Segalen et al., 2010), we found that it cannot orient the spindle on its own (Fig. 1d), suggesting that there may be spindle orientation activity within the adjacent C-terminal (CT) domain. The CT domain following the DEP domain has no characterized function in spindle orientation and also fails to orient the spindle when examined alone, indicating that both DEP and CT domains are necessary for Dsh activity (Fig. 1e). Sequence analysis of the CT domain revealed several low-complexity motifs and low overall multi-sequence conservation. Thus, as an unbiased approach to identifying the sequence in the Dsh CT that cooperates with the DEP domain, we analyzed iterative deletions of the CT region. We found that residues at the extreme COOH-terminus are required for DEP-CT spindle orientation activity (Fig. 1e; Supplemental Figure 1a-e); more internal CT deletions did not further impair activity. The final ten CT residues resemble a PDZ domain ligand sequence and residues important for interaction with PDZ domains are conserved (Supplemental Figure 1). Direct fusion of this putative PDZ ligand (PDZL) with the DEP domain was sufficient for complete spindle orientation (Fig. 1f). Thus, the Dsh COOH terminus, which has no previously known spindle orientation activity, functions synergistically with the DEP domain for robust spindle alignment (Fig. 1g).

To identify potential effectors of the Dsh COOH-terminus, we first surveyed known spindle orientation components containing PDZ domains, such as the scaffold proteins Discs large (Dlg) and Canoe (Cno; AF-6/Afadin in vertebrates) (Johnston et al., 2009; Siegrist and Doe, 2005; Speicher et al., 2008; Wee et al., 2011). We have previously shown that loss of Dlg does not prevent Dsh-mediated spindle orientation (Segalen et al., 2010). However, Cno RNAi completely blocked Ed:DEP-CT spindle orientation (Fig. 2a). Pulldown experiments with purified components identified a direct interaction between the Dsh COOH-terminus and Cno^{PDZ} *in vitro* (Fig. 2b), which is in general agreement with a previous report (Carmena et al., 2006), and indicates that the COOH-terminus is indeed a PDZ ligand (PDZL). Consistent with a direct interaction

between Dsh and Cno, HA:Cno^{PDZ} is recruited to cortical crescents of Ed:DEP-CT (Fig. 2c,d). We conclude that Cno acts as a proximal effector in the Dsh^{PDZL} spindle orientation pathway through a canonical PDZ interaction.

How might Cno function in Dsh-mediated spindle orientation? Cno is also required for Pins/Mud/dynein-mediated spindle orientation (Carmena et al., 2011; Speicher et al., 2008; Wee et al., 2011). The Pins TPR domain binds Mud in a manner analogous to the Dsh DEP domain (Nipper et al., 2007; Smith and Prehoda, 2011). Loss of Cno prevents Pins-Mud association in both neuroblasts and S2 cells (Speicher et al., 2008; Wee et al., 2011), so we tested whether Cno is required for Dsh-Mud association. We assayed for the ability of Ed:DEP-CT to recruit Mud in the absence of Cno, but found that Cno was not required for Ed:DEP-CT to recruit Mud (Fig. 2e-g). Thus, while Cno functions to mediate Mud interaction with Pins, it is not required for Mud binding to Dsh, but is nevertheless required for Dsh-mediated spindle orientation. The Pins/Mud pathway, initiated by the Pins TPR domain, functions synergistically with a pathway downstream of the Pins Linker domain that couples to the kinesin Khc73 (Johnston et al., 2009; Siegrist and Doe, 2005). To determine if Khc73 also cooperates with Dsh/Mud, we examined Ed:Dsh spindle orientation in cells treated with RNAi directed against Khc73 and observed no effect (Supplementary Fig. 2a), further supporting the role for a novel pathway involving the Dsh^{PDZL}/Canoe complex.

The Dsh^{PDZL}/Canoe complex has no previously characterized function in spindle orientation, appears to operate distinctly from the Pins^{Linker}/Dlg/Khc73 pathway, and does not affect Dsh/Mud cortical association (Fig. 2e-g). To gain insight into its molecular function, we next sought to identify the components that act downstream of the Dsh^{PDZL}/Cno module. The Dsh CT is thought to constitute the main hub for 'non-canonical' Dsh signaling, which is mainly comprised of Rho and Rac GTPase signaling pathways (Malbon and Wang, 2006). Moreover, Canoe acts upstream of Rho superfamily GTPase signaling in other systems (Miyata et al., 2009; Slovakova et al., 2012), and Rho has recently been identified as a regulator of spindle orientation by Anthrax toxin receptor in zebrafish (Castanon et al., 2012). Treatment of S2 cells with RNAi against Rac, or its key effector JNK, did not affect alignment of the spindle to polarized Dsh (Supplemental Figure 2b). Rho-targeted RNAi, however, completely abolished Dsh-mediated spindle orientation (Fig. 3a). Rho RNAi was specific to the Dsh pathway, as it had no effect on Pins-mediated spindle orientation (Fig. 3b). Moreover, no significant alterations in cell or spindle morphology were observed following Rho RNAi treatment. Overexpression of a dominant-negative Rho mutant also prevents Dsh activity (Fig. 3c,d). These data show that Rho is not part of a common Mud/dynein spindle orientation pathway, and that loss of Rho does not lead to pleiotropic cell or spindle defects that preclude spindle orientation. We conclude that a Rho-dependent spindle orientation pathway functions downstream of the Dsh C-terminal domain.

Rho normally resides in an inactive, GDP-bound conformation and becomes activated by guanine nucleotide exchange factors (GEFs), allowing for spatiotemporal regulation of signaling (Mulinari and Hacker, 2010). A RhoGEF2/Rho signaling pathway has been shown to regulate several key morphogenic events during *Drosophila* development, including cellularisation, epithelial invagination, and gastrulation (Barrett et al., 1997; Grosshans et al., 2005; Kolsch et al., 2007; Simoes et al., 2006). Moreover, RhoGEF2, which contains two -SxIP- motifs (Honnappa et al., 2009), localizes to

microtubule plus-ends by interaction with EB-1 (Rogers et al., 2004), a known regulator of spindle orientation (Rogers et al., 2002; Toyoshima and Nishida, 2007). Plus-end microtubule localization of RhoGEF2 could allow for spatially controlled cortical Rho activation during spindle orientation. We found that RNAi targeted against RhoGEF2 or EB-1 resulted in loss of spindle orientation by cortically polarized Dsh (Fig. 3e,f). RNAi directed against RhoGEF4, an unrelated GEF with no known microtubule localization had no effect (Supplemental Figure 2c). We conclude that Rho GTPase and its activator, RhoGEF2, are required for Dsh-mediated spindle orientation.

We next sought to identify the Rho effector that might regulate spindle orientation. Rho kinase (ROK) is a key Rho effector and regulates several Rho-mediated morphogenic events, including spindle orientation by Antxr2a (Amano et al., 2010). However, RNAi knockdown of ROK had no significant effect on Dsh-mediated spindle orientation (Supplemental Figure 2d). An alternative Rho effector acting in non-canonical Dsh signaling is the formin protein family, which also mediates Antxr2a spindle orientation (Malbon and Wang, 2006). Binding of active Rho relieves an autoinhibitory formin conformation, thereby enhancing its polymerization activity on the fast-growing, barbed end of actin filaments (Otomo et al., 2005). RNAi targeted against the formin Diaphanous (Dia) completely abolished Dsh-mediated spindle orientation (Fig. 4a). Identical Dia RNAi treatment had no effect on Pins-mediated spindle orientation (Fig. 4b), illustrating the Dsh-specific nature of this pathway. Moreover, expression of GFP:Dia showed robust recruitment specifically to Dsh cortical crescents (Fig. 4c,d,f). Dia recruitment was significantly reduced following treatment with Cno RNAi, which places Dia downstream of the Dsh^{PDZL} pathway (Fig. 4e,f). The actin polymerizing function of Dia depends on its FH1 domain interaction with Profilin, known as Chickadee (Chic) in *Drosophila*. Chic binds and recruits monomeric actin molecules that are integrated into the growing actin filament by the action of the Dia FH2 domain(Chesarone et al., 2010). Chic RNAi also blocks Dsh-mediated spindle orientation (Fig. 4f), suggesting that the effects of Dia RNAi are indeed caused by defects in actin polymerization. Interestingly, cells depleted of Arp2, a component of the Arp2/3 complex, displayed normal spindle orientation (Fig. 4g-i). Arp2/3 nucleates newly branched actin networks by binding the side of a mother filament (Campellone and Welch, 2010), as opposed to formin-mediated elongation of existing filaments. Taken together, these results suggest that Dsh-mediated spindle orientation – but not Pins-mediated spindle orientation – requires nucleation of linear F-actin.

Several studies have demonstrated an actin-independent role of Dia in microtubule stabilization (Bartolini et al., 2008; Palazzo et al., 2001), which could play a role in spindle orientation (Pease and Tirnauer, 2011). Although the requirement for Chic suggested that the essential function of Dia is filament nucleation, to further test this model we assayed the spindle orientation activity of a Dia point mutant (I690A) that is defective in actin polymerization but retains microtubule stabilization function (Bartolini et al., 2008). Wild type or I690A forms of GFP:Dia were expressed in cells previously treated with a Dia RNAi construct targeted against the 5'-UTR to deplete endogenous Dia. Whereas wild type Dia fully rescued the effects of RNAi (Fig. 5a), spindle orientation in the I690A Dia expressing cells remained randomized. This lack of rescue was despite proper recruitment of Dia I690A to the Dsh cortical crescent (Fig 5b), suggesting Dia localization is independent of actin nucleation. We conclude that

Dsh-mediated spindle orientation requires the Dia-induced nucleation of linear actin filaments.

To directly visualize the effects of Dsh on cortical actin polymerization, we stained cells with dye-conjugated phalloidin. In Ed alone control cells, cortical actin staining varied in intensity but was typically equally distributed cortically or less intense at cell contacts (Fig. 5c,f). Expression of Ed:Dsh resulted in asymmetric phalloidin staining, with intense signal coinciding along the entire Ed:Dsh crescent, indicating a Dsh-mediated increase in cortical actin polymerization (Fig. 5d,f). Treatment with Dia RNAi abolished this asymmetry, leading to F-actin staining similar to cells expressing Ed alone (Fig. 5e,f). Importantly, Dia RNAi did not result in global actin polymerization defects as symmetric cortical actin staining can still be seen similar to control cells. We conclude that Dsh localizes and activates Dia to induce asymmetric cortical actin polymerization necessary for proper spindle orientation.

To determine if this actin-based Dsh spindle orientation pathway is active during *Drosophila* development we assayed sensory organ precursor (SOP) cell divisions. Our work and others have shown that SOP cell division requires both Dsh- and Pins-mediated spindle orientation pathways: Dsh regulates spindle orientation along the anterior-posterior axis, whereas Pins orients the spindle along the apical-basal axis (David et al., 2005; Gho and Schweisguth, 1998; Segalen et al., 2010). We expressed UAS-Dia, -RhoGEF2, or -Rho RNAi constructs specifically in pI cells using the Neuralized-GAL4 line and examined spindle orientation in 16-hour pupae. Expression of RhoGEF2- or Rho-RNAi resulted in embryonic lethality prohibiting examination. Expression of Dia-RNAi resulted in significantly reduced spindle orientation relative to the A-P body axis (Fig. 6a,b). In contrast, Dia-RNAi did not affect spindle orientation relative to Pins crescents (Fig. 6b'). We conclude that the Dsh/Dia spindle orientation pathway is required for anterior-posterior spindle orientation in the SOP lineage, and that Dia acts specifically in the Dsh but not Pins spindle orientation pathways in vivo, confirming to our observations in the S2 spindle orientation assay.

Although Pins does not require Dia for apical-basal spindle orientation, Pins-mediated spindle orientation does require a secondary pathway to cooperate with Mud/Dynein. While the $Pins^{TPR}$ domain uses Mud/Dynein analogously to Dsh^{DEP}, the $Pins^{Linker}$ functions via the kinesin Khc73, and both pathways are required for spindle positioning (Fig. 7a,b). Whereas the Dsh^{PDZL}/Dia and $Pins^{Linker}$/Khc73 pathways result in very different endpoints, linear actin filament nucleation and microtubule motor activity, respectively, we asked whether they could function interchangeably. We generated chimeras that pair Pins with the Dia pathway ($Pins^{TPR}$+Dsh^{PDZL}), and Dsh with the Khc73 pathway (Dsh^{DEP}+$Pins^{Linker}$). Both chimeric proteins had robust spindle orientation activity (Fig. 7c). These results indicate that the accessory pathways that operate with Pins TPR/Mud and Dsh DEP/Mud, while using very distinct components, can function in a modular fashion.

DISCUSSION

While PCP is critical for development and homeostasis, relatively little is known about how the Fz/Dsh PCP pathway positions the spindle. We recently identified Mud/Dynein as a critical component of Dsh-mediated spindle orientation in flies and zebrafish (Segalen et al., 2010). In the present work we identify a new pathway that cooperates

with Mud/Dynein by regulating cortical F-actin. This pathway is initiated by a PDZ ligand sequence at the Dsh C-terminus, which binds directly to Canoe, a known spindle orienting protein. The Dsh C-terminal pathway is regulated by the Rho GTPase, a direct activator of the formin Dia whose actin nucleating activity is critical for spindle orientation. Thus, we have identified the upstream elements that initiate this new pathway (Dsh C-term and Canoe), and actin filament regulators that carry out its function (RhoGEF2, Rho, Dia, and Chic).

Some of the components in the Dsh C-term pathway (e.g. Rho) are broad regulators of cellular function, suggesting that their requirement for spindle orientation may not be specific. However, we examined each pathway component in both Dsh and Pins-mediated spindle orientation to determine the degree with which each is required specifically for spindle orientation by Dsh. Canoe is known to regulate spindle alignment to cortical Pins, and we have found that it binds directly to Dsh and also regulates the PCP pathway. In contrast to Canoe, however, the remaining components that we identified are specific to the Dsh PCP pathway. Interestingly, we also found that chimeras of Pins and Dsh orient the spindle, demonstrating that the kinesin (Khc73) pathway used by Pins and the formin (Dia) Dsh pathway are functionally interchangeable. Thus, while each pathway appears to have very different molecular functions, they are nevertheless able to combine with Mud/Dynein to achieve robust spindle alignment in our assays.

How might formin-induced linear actin polymerization contribute to Fz/Dsh spindle positioning? In budding yeast, the formin Bni1 nucleates linear actin cables to guide astral microtubule plus ends into the emerging bud (Lee et al., 1999; Ten Hoopen et al., 2012). However, this process is very different from metazoan spindle orientation in which the spindle becomes aligned before telophase. Metazoans also lack several of the key components that link F-actin to astral microtubules in yeast. Studies in animal cell models have suggested an indirect role for F-actin, as it is required for establishment and maintenance of cell polarity factors that subsequently influence spindle positioning (Kunda and Baum, 2009). A potentially more direct role has been demonstrated in integrin-mediated spindle orientation, which uses the actin network to link spindle microtubules to the extracellular adhesion matrix (Toyoshima and Nishida, 2007). Although this pathway depends on both cortical actin and EB-1, also identified downstream of Dsh here, it relies on distinct regulatory components such as myosin-X, Cdc42, and phosphoinositides (Mitsushima et al., 2009; Toyoshima et al., 2007; Toyoshima and Nishida, 2007). Thus, different cortical cues appear to utilize actin nucleation for spindle orientation through diverse mechanisms. Nevertheless, studies have shown that cortical actin substructures can exert forces that induce spindle orientation (Fink et al., 2011), which could present common output of each upstream pathway.

The recruitment of Dia and enrichment of F-actin at sites of Ed-Dsh indicates that formins contribute to spindle orientation by regulating cortical F-actin. Very recent studies of the Antxr2 receptor during oriented divisions of zebrafish epiblasts have also identified a necessary role for Dia, although it remains uncertain if Antxr2a-mediated spindle orientation is strictly dependent on actin nucleation (Castanon et al., 2012). Interestingly, Dsh-mediated actin nucleation is required for Antxr2 cortical localization, although actin polymerization is regulated by ROK downstream of Dsh in this system.

Thus, Dsh appears to regulate cortical actin via diverse, cell specific signaling pathways to elicit spindle orientation. Future studies will be needed to identify the actin-associated regulators involved in coupling cortical actin to spindle microtubules and how these connections dictate spindle orientation.

METHODS

Reagents and antibodies.

Chemicals and standard reagents were purchased from Sigma Aldrich (St. Louis, MO) unless otherwise noted. Antibodies used were as follows: rat α-tubulin, 1:1000 (Abcam); mouse α-tubulin, 1:1000 (DM1A, Sigma); rabbit HA, 1:1000 (Covance); rabbit ROK, 1:1000 (Sigma); goat Arp2, 1:1000 (Santa Cruz); rabbit phosphohistone-3, 1:1500 (Upstate); rat Pins, 1:400(Yu et al., 2000); guinea pig senseless, 1:3000 (generous gift from H. Bellen); HRP-linked secondary antibodies (Promega), Alexa dye-linked secondary antibodies (Jackson Laboratories).

Cell culture, plasmid transfection, and RNAi.

Drosophila S2 cells were maintained and passaged as required in Schneider insect media (SIM) supplemented with 10% fetal bovine serum. All plasmids were constructed in the copper-inducible pMT-V5 vector (Invitrogen, Carlsbad, CA). Ed fusion constructs were engineered as previously described (Johnston et al., 2009). For transient expression, S2 cells were plated in 6-well culture dishes at a density of ~1-3 × 10^6 cells per well and transfected with 0.5 μg of individual plasmids using the Effectene reagent (QIAGEN, Germantown, MD). After ~36 hours, protein expression was induced by addition of 500 μM $CuSO_4$ for ~24 hours.

For RNAi experiments, cells were transfected as described. After ~36 hours, cells were harvested and resuspended in serum-free media to a density of ~1 × 10^6 cells per well (1 mL volume per well). Cells were incubated with 10 μg of RNAi for 1 hour and 2 mL of serum-containing media was added. Following a 3-day incubation, copper sulfate was added as described. All RNAi primers were designed using the SnapDragon online tool (http://www.flyrnai.org/cgi-bin/RNAi_find_primers.pl) and included T7 promoter tags. PCR-amplified fragments were reverse transcribed and dsRNAi was isolated using the MegaScript T7 kit (Ambion, Austin, TX).

The ‘induced polarity’ Ed assay has been previously described (Johnston et al., 2009). Briefly, following $CuSO_4$ induction, cell clusters were formed by agitation of cells on a platform shaker at ~175 RPM for 1 hour. Cells were then plated on individual coverslips for 2-3 hours in fresh media to increase the mitotic index. Cells were washed with PBS and fixed in 3% paraformaldehyde for 15 min. Cells were then washed (PBS + 0.1% saponin) and blocked for 1 hour (wash buffer + 1% BSA). Primary antibodies were added overnight at 4C. Washed cells were then incubated with secondary antibodies for 2 hours at room temperature, washed again, and mounted. All images were acquired using a Leica SP2 confocal microscope with a 60× 1.4 NA lens. Spindle angles were measured by two lines made through a single confocal section containing both spindle asters, one line formed between the center of the Ed signal at the cell cortex and the

center of the cell, and the other along the axis of the spindle. The ImageJ angle function was used for the measurement.

Several phenotypic aspects of the 'induced polarity' Ed assay are carefully controlled in all experiments. First, S2 cells have been documented to present variations in spindle size, morphology, centrosomes, and tubulin staining intensities (Goshima and Vale, 2003; Morales-Mulia and Scholey, 2005). To prevent potential nonspecific effects due to these variations, we disregard cells with multipolar or bent/broken spindle morphologies, although minor deviations in spindle focusing is tolerated equally across experimental conditions. Images presented in figures are selected to represent the average phenotype demonstrated for each condition. Second, while variations in crescent sizes are expected, we ensure that for selected cells crescents fall within a 60° cortical range. This prevents sampling cells containing large crescents that could likely introduce a skew toward larger angle measurements. Average crescents sizes closely reflect those seen in numerous polarized cells *in vivo*, including SOPs examined herein. Finally, in addition to their cortical localization, transfected Ed fusion proteins often demonstrate cytoplasmic expression in the form of small puncta. The degree of these cytoplasmic punta do not differ among experimental conditions, and we have previously shown that spindle orientation is not affected by their presence (Johnston et al., 2009).

For phalloidin staining, cells were plated on glass coverslips previously treated with Concanavalin-A (0.5 mg/ml for 1 hour; air dried overnight). Following fixation as above, cells were neutralized in 10 mM ethanolamine for 5 min and subsequently permeablized by incubation in 0.1% Triton X-100 in PBS. Alexa fluor®-555 phalloidin (Invitrogen) was added for 20 min, after which cells were rinsed in PBS and mounted. Quantification of cortical phalloidin intensity was conducted using ImageJ software. Briefly, the Ed:GFP channel of each image was used to identify the 'crescent' and 'noncrescent' cortical regions, which were individually traced using the 'polygon selection' tool in ImageJ. Average intensities of phalloidin staining within each region were then quantified and crescent:noncrescent ratios were documented. Statistical comparisons were made with ANOVA in GraphPad Prism software. Similar procedures were carried out for quantifying cortical localization to Ed crescents of expressed constructs (*e.g.* GFP:Dia).

GST pulldowns and immunoblotting.
All recombinant proteins were produced in *E. coli* (BL21-DE3) and purified by sequential affinity, ion exchange, and size exclusion chromatography as described elsewhere (Johnston et al., 2009). For pulldowns, clarified *E. coli* lysates expressing GST fusions were incubated with glutathione-agarose beads (Sigma) for 1 hour at room temperature in PBS. Beads were extensively wash and resuspended in buffer (20 mM Tris [pH 7.5], 250 mM NaCl, 5 mM $MgCl_2$, 0.5 mM EDTA, 1 mM DTT, and 1.5% Triton X-100). Prey proteins (50 μg) were added and reactions were rotated at 4°C for 2 hours. Beads were extensively washed and beads were eluted in boiling loading buffer for 5 min. Equal volumes were analyzed by SDS-PAGE electrophoresis and transferred to nitrocellulose membranes for western blot detection.

***Drosophila* genetics and dissection.**

Stocks used were as follows: *w;neur[Gal4-A101], Kg[V]/TM3, Sb* (Bloomington Stock Center); *UAS-dia-RNAi*, homozygous hairpin insertion on chromosome II (VDRC Stock Center, ID: 103914). Crosses of *Neur[Gal4-A101], Kg[V]* × *UAS-Diaph-RNAi* were raised 25°C. White pupae were harvested from experimental *UAS-Diaph-RNAi /+ ; Neur[Gal4-A101], Kg[V]/+* and the sibling controls *UAS-Diaph-RNAi /+ ; TM3,Sb/+* and aged to 16 hours APF at 25°C on damp filter paper in glass vials. Pupae were then dissected in PBS, followed by immediate fixation for 20 min in PBS with 4% paraformaldehyde, 0.3% Triton, 2% DMSO. Samples were then blocked overnight at 4°C in PBS supplemented with 4% FBS, 0.1% Triton, and 10mM glycine. Primary and secondary antibodies diluted in blocking solution were applied for 1 hour at room temperature. Samples were rinsed twice in blocking solution followed by two rinses in glycerol (25% and 50% for 10 minutes each). A final wash (90% glycerol with 2% N-Propyl gallate for antifade properties) was done and samples were mounted. All fluorescent images were collected on a Bio-Rad Radiance 2100MP confocal and Nikon E600FN Upright microscope.

ACKNOWLEDGEMENTS
The authors would like to thank B. Nolen for supplying the Arp2 antibody and members of the Doe and Prehoda laboratories for helpful comments and suggestions. This work was supported by a grant from the NIH (5R01GM087457, K.E.P.) and the Howard Hughes Medical Institute (C.Q.D.) and the Damon Runyon Cancer Foundation (C.A.J.).

AUTHOR CONTRIBUTIONS
C.A.J., K.E.P., and C.Q.D. conceived the experiments and prepared the manuscript. C.A.J. conducted the majority of the experiments; L.M. carried out the genetics and imaging of *Drosophila* SOPs. M.S.L. conducted Dia localization experiments. O.G. conducted deletion experiments involving the Dsh CT domain. C.Q.D. and K.E.P. directed the research program.

COMPETING FINANCIAL INTERESTS
The authors declare no competing financial interests.

FIGURE LEGENDS

Figure 1 The Dsh DEP domain functions with ten residues at its COOH-terminus to orient the mitotic spindle. (**a**) Dsh domain architecture. (**b**) Measurement of spindle angle, α, relative to Ed fusion. (**c-f**) Representative images for each experiment are shown along with the distribution of observed spindle angles. Echinoid fusions to Dsh are shown in green; tubulin is shown in red. (**g**) Comparison of Pins- and Dsh-mediated spindle orientation. Full spindle orientation by Pins requires both Mud/Dynein and Khc73 pathways, whereas Dsh requires Mud/Dynein and a pathway downstream of its PDZL.

Figure 2 The Dsh PDZL binds and recruits Canoe/Afadin to orient the spindle. (**a**) Representative image for S2 cell treated with Cno RNAi and expressing Ed:DEP-CT. The distribution of observed spindle angles for these cells is also shown. (**b**) The Dsh^{PDZL} interacts directly with Cno^{PDZ}. GST:Dsh^{PDZL} adsorbed on glutathione agarose precipitates a Maltose Binding Protein (MBP) fusion of Cno^{PDZ}. Ponceau stained nitrocellulose shows total protein (left), while an anti-MBP western shows the Cno^{PDZ}. (**c**) Ed does not recruit Cno^{PDZ}. S2 cells flattened on Con A coated slides and expressing Ed and an HA fusion of Cno^{PDZ}. (**d**) DEP-CT recruits Cno^{PDZ}. S2 cells adhered on Con A coated slides and expressing Ed:DEP-CT and an HA fusion of Cno^{PDZ}. (**e**) DEP-CT recruits Mud. S2 cells in suspension recruit endogenous Mud. (**f**) Loss of Cno has no effect on DEP-CT recruitment of Mud. S2 cells cultured in suspension and treated with Cno RNAi as in panel 'a' also recruit endogenous Mud. (**g**) Quantification of localization from panels c-e. Asterisks denote statistical significance evaluated by 1 way ANOVA with Dunnet's post test (* denotes $p < 0.05$; ** denotes $p < 0.01$)

Figure 3 Rho, RhoGEF2, and EB-1 are required for Dsh-mediated spindle orientation. (**a-f**) Representative images are displayed for indicated RNAi treatments in either Ed:Dsh (DEP-CT)- or Ed:Pins-expressing cells. The distributions of spindle angles observed for cells in each of the conditions are also shown. In addition to Ed:DEP-CT, the experiments depicted in panels c and d include expression of HA fused WT or dominant negative (T19N) Rho.

Figure 4 The formin Diaphanous and its cofactor profilin act downstream of Canoe in Dsh-mediated spindle orientation. (**a**) Dia is required for Dsh (Ed:DEP-CT) spindle orientation. A representative image is shown along with the distribution of observed spindle angles. (**b**) Dia is not required for Ed:Pins-mediated spindle orientation. Data are shown as in panel a. (**c-e**) Dia recruitment to Ed:DEP-CT requires Cno. S2 cells adhered on ConA-coated slides expressing the indicated Ed fusion and GFP-Dia are shown. (**f**) Quantification of localization results in panels c-e. Asterisks denote statistical significance evaluated by 1 way ANOVA with Dunnet's post test (* denotes $p < 0.05$; ** denotes $p < 0.01$). (**g**) The *Drosophila* profilin Chicadee (Chic) is required for Dia-mediated spindle orientation. Data are shown as in panel a. (**h**) The branched actin filament nucleator Arp2/3 is not required for Dsh-mediate spindle orientation. Data are shown as in panel a. (**i**) A western blot showing the efficiency of Arp2 knockdown is shown with αTubulin as a loading control.

Figure 5 Dia spindle orientation function requires its actin filament nucleation activity (**a**) Representative images indicating the ability of GFP-Dia wild-type (WT) or (**b**) an actin polymerization-deficient mutant (I690A) to rescue the loss of spindle orientation resulting from RNAi directed against the 5'-UTR of endogenous Dia in S2 cells. Localization of each GFP:Dia construct is shown in the grey insets; note the I690A mutant retains proper membrane recruitment to Ed:DEP-CT. The distribution of observed spindle angles is also shown for each condition. (**c-e**) Cortical Dsh leads to Dia-dependent cortical actin enrichment. S2 cells adhered on ConA-coated slides expressing the indicated Ed fusion and treated with Dia RNAi (panel e) are shown. (**f**) Quantification of localization results in panels c-e. Asterisks denote statistical significance evaluated by 1 way ANOVA with Dunnet's post test (* denotes $p < 0.05$; ** denotes $p < 0.01$).

Figure 6 Dia is required for proper anterior-posterior orientation of pI cell divisions in *Drosophila* imaginal discs. Cell-specific expression of UAS-Dia was achieved using the Neuralized-GAL4 driver. Senseless marker staining (red) confirmed identity of pI cells, and UAS-Dia expressing or control sibling pupae were analyzed. (**a**) Spindle orientation is shown relative to the A-P axis of the animal; (**a'**) Spindle orientation relative to Pins. (**b**) Spindle orientation relative to the A-P axis in SOP cells expressing Dia RNAi; (**b'**) Spindle orientation relative to Pins indicating that orientation relative to this intrinsic cue is not disrupted by Dia RNAi. Representative images are displayed along with the distribution of observed spindle angles relative to A-P axis.

Figure 7 Spindle orientation requires Mud/Dynein and an accessory pathway. (**a**) Comparison of Pins- and Dsh-mediated spindle orientation. Each utilizes a common pathway (Mud/Dynein) and very distinct secondary pathways (Khc73 for Pins, and Dia for Dsh). (**b**) Pins and Dsh chimeras are functional. Echinoid fusions of proteins that combine the Dsh^{DEP} and $Pins^{Linker}$ domains, or the $Pins^{TPR}$ and Dsh^{PDZL} efficiently orient the spindle.

Figure S1 The Dsh DEP domain requires residues at the COOH-terminus to orient the mitotic spindle. (**a**) Dsh DEP-CT domain architecture. (**b-e**) Representative images for each experiment are shown along with the distribution of observed spindle angles. Echinoid fusions to Dsh are shown in red; tubulin is shown in green. (**f**) Sequence alignment of the Dsh COOH-terminus reveals a putative PDZ ligand domain conserved across all metazoans. NCBI accession numbers: *H.sapiens* – AAB47447.1, *G.gallus* – XP_422756.3, *D.rerio* – NP_997813.1, *X.laevis* – NP_001084096.1, *C.intestinalis* – NP_001027754.1, *C.gigas* – EKC26253.1, *T.castaneum* – XP967594.1, *A.pisum* – XP_003247704.1, *A.queenslandica* – XP_003384321.1, *D.melanogaster* – AAF48033.1

Figure S2 RNAi against other potential signaling components does not prevent Dsh-mediated spindle orientation. S2 cells expressing Ed:DEP-CT were treated with RNAi directed against Khc73 (**a**), Rac (**b**), JNK (**c**), RhoGEF4 (**d**), or ROK (**e**) and spindle orientation was assessed. For ROK, western blot antibody detection indicates robust knockdown of protein expression.

References

Amano, M., Nakayama, M. and Kaibuchi, K. (2010). Rho-kinase/ROCK: A key regulator of the cytoskeleton and cell polarity. *Cytoskeleton (Hoboken)* 67, 545-54.

Barrett, K., Leptin, M. and Settleman, J. (1997). The Rho GTPase and a putative RhoGEF mediate a signaling pathway for the cell shape changes in Drosophila gastrulation. *Cell* 91, 905-15.

Bartolini, F., Moseley, J. B., Schmoranzer, J., Cassimeris, L., Goode, B. L. and Gundersen, G. G. (2008). The formin mDia2 stabilizes microtubules independently of its actin nucleation activity. *J Cell Biol* 181, 523-36.

Bowman, S. K., Neumuller, R. A., Novatchkova, M., Du, Q. and Knoblich, J. A. (2006). The Drosophila NuMA Homolog Mud regulates spindle orientation in asymmetric cell division. *Dev Cell* 10, 731-42.

Campellone, K. G. and Welch, M. D. (2010). A nucleator arms race: cellular control of actin assembly. *Nat Rev Mol Cell Biol* 11, 237-51.

Carmena, A., Makarova, A. and Speicher, S. (2011). The Rap1-Rgl-Ral signaling network regulates neuroblast cortical polarity and spindle orientation. *J Cell Biol* 195, 553-62.

Carmena, A., Speicher, S. and Baylies, M. (2006). The PDZ protein Canoe/AF-6 links Ras-MAPK, Notch and Wingless/Wnt signaling pathways by directly interacting with Ras, Notch and Dishevelled. *PLoS One* 1, e66.

Castanon, I., Abrami, L., Holtzer, L., Heisenberg, C. P., van der Goot, F. G. and Gonzalez-Gaitan, M. (2012). Anthrax toxin receptor 2a controls mitotic spindle positioning. *Nat Cell Biol*.

Chesarone, M. A., DuPage, A. G. and Goode, B. L. (2010). Unleashing formins to remodel the actin and microtubule cytoskeletons. *Nat Rev Mol Cell Biol* 11, 62-74.

David, N. B., Martin, C. A., Segalen, M., Rosenfeld, F., Schweisguth, F. and Bellaiche, Y. (2005). Drosophila Ric-8 regulates Galphai cortical localization to promote Galphai-dependent planar orientation of the mitotic spindle during asymmetric cell division. *Nat Cell Biol* 7, 1083-90.

Fink, J., Carpi, N., Betz, T., Betard, A., Chebah, M., Azioune, A., Bornens, M., Sykes, C., Fetler, L., Cuvelier, D. et al. (2011). External forces control mitotic spindle positioning. *Nat Cell Biol* 13, 771-8.

Gho, M. and Schweisguth, F. (1998). Frizzled signalling controls orientation of asymmetric sense organ precursor cell divisions in Drosophila. *Nature* 393, 178-81.

Goshima, G. and Vale, R. D. (2003). The roles of microtubule-based motor proteins in mitosis: comprehensive RNAi analysis in the Drosophila S2 cell line. *J Cell Biol* 162, 1003-16.

Grosshans, J., Wenzl, C., Herz, H. M., Bartoszewski, S., Schnorrer, F., Vogt, N., Schwarz, H. and Muller, H. A. (2005). RhoGEF2 and the formin Dia control the formation of the furrow canal by directed actin assembly during Drosophila cellularisation. *Development* 132, 1009-20.

Honnappa, S., Gouveia, S. M., Weisbrich, A., Damberger, F. F., Bhavesh, N. S., Jawhari, H., Grigoriev, I., van Rijssel, F. J., Buey, R. M., Lawera, A. et al. (2009). An EB1-binding motif acts as a microtubule tip localization signal. *Cell* 138, 366-76.

Johnston, C. A., Hirono, K., Prehoda, K. E. and Doe, C. Q. (2009). Identification of an Aurora-A/PinsLINKER/Dlg spindle orientation pathway using induced cell polarity in S2 cells. *Cell* 138, 1150-63.

Kolsch, V., Seher, T., Fernandez-Ballester, G. J., Serrano, L. and Leptin, M. (2007). Control of Drosophila gastrulation by apical localization of adherens junctions and RhoGEF2. *Science* 315, 384-6.

Kunda, P. and Baum, B. (2009). The actin cytoskeleton in spindle assembly and positioning. *Trends Cell Biol* 19, 174-9.

Lee, L., Klee, S. K., Evangelista, M., Boone, C. and Pellman, D. (1999). Control of mitotic spindle position by the Saccharomyces cerevisiae formin Bni1p. *J Cell Biol* 144, 947-61.

Malbon, C. C. and Wang, H. Y. (2006). Dishevelled: a mobile scaffold catalyzing development. *Curr Top Dev Biol* 72, 153-66.

Mitsushima, M., Toyoshima, F. and Nishida, E. (2009). Dual role of Cdc42 in spindle orientation control of adherent cells. *Mol Cell Biol* 29, 2816-27.

Miyata, M., Rikitake, Y., Takahashi, M., Nagamatsu, Y., Yamauchi, Y., Ogita, H., Hirata, K. and Takai, Y. (2009). Regulation by afadin of cyclical activation and inactivation of Rap1, Rac1, and RhoA small G proteins at leading edges of moving NIH3T3 cells. *J Biol Chem* 284, 24595-609.

Morales-Mulia, S. and Scholey, J. M. (2005). Spindle pole organization in Drosophila S2 cells by dynein, abnormal spindle protein (Asp), and KLP10A. *Mol Biol Cell* 16, 3176-86.

Morin, X. and Bellaiche, Y. (2011). Mitotic spindle orientation in asymmetric and symmetric cell divisions during animal development. *Dev Cell* 21, 102-19.

Mulinari, S. and Hacker, U. (2010). Rho-guanine nucleotide exchange factors during development: Force is nothing without control. *Small GTPases* 1, 28-43.

Nipper, R. W., Siller, K. H., Smith, N. R., Doe, C. Q. and Prehoda, K. E. (2007). Galphai generates multiple Pins activation states to link cortical polarity and spindle orientation in Drosophila neuroblasts. *Proc Natl Acad Sci U S A* 104, 14306-11.

Otomo, T., Otomo, C., Tomchick, D. R., Machius, M. and Rosen, M. K. (2005). Structural basis of Rho GTPase-mediated activation of the formin mDia1. *Mol Cell* 18, 273-81.

Palazzo, A. F., Cook, T. A., Alberts, A. S. and Gundersen, G. G. (2001). mDia mediates Rho-regulated formation and orientation of stable microtubules. *Nat Cell Biol* 3, 723-9.

Pease, J. C. and Tirnauer, J. S. (2011). Mitotic spindle misorientation in cancer--out of alignment and into the fire. *J Cell Sci* 124, 1007-16.

Rogers, S. L., Rogers, G. C., Sharp, D. J. and Vale, R. D. (2002). Drosophila EB1 is important for proper assembly, dynamics, and positioning of the mitotic spindle. *J Cell Biol* 158, 873-84.

Rogers, S. L., Wiedemann, U., Hacker, U., Turck, C. and Vale, R. D. (2004). Drosophila RhoGEF2 associates with microtubule plus ends in an EB1-dependent manner. *Curr Biol* 14, 1827-33.

Segalen, M., Johnston, C. A., Martin, C. A., Dumortier, J. G., Prehoda, K. E., David, N. B., Doe, C. Q. and Bellaiche, Y. (2010). The Fz-Dsh planar cell polarity pathway

induces oriented cell division via Mud/NuMA in Drosophila and zebrafish. *Dev Cell* 19, 740-52.

Siegrist, S. E. and Doe, C. Q. (2005). Microtubule-induced Pins/Galphai cortical polarity in Drosophila neuroblasts. *Cell* 123, 1323-35.

Siller, K. H., Cabernard, C. and Doe, C. Q. (2006). The NuMA-related Mud protein binds Pins and regulates spindle orientation in Drosophila neuroblasts. *Nat Cell Biol* 8, 594-600.

Siller, K. H. and Doe, C. Q. (2009). Spindle orientation during asymmetric cell division. *Nat Cell Biol* 11, 365-74.

Simoes, S., Denholm, B., Azevedo, D., Sotillos, S., Martin, P., Skaer, H., Hombria, J. C. and Jacinto, A. (2006). Compartmentalisation of Rho regulators directs cell invagination during tissue morphogenesis. *Development* 133, 4257-67.

Slovakova, J., Speicher, S., Sanchez-Soriano, N., Prokop, A. and Carmena, A. (2012). The actin-binding protein Canoe/AF-6 forms a complex with Robo and is required for Slit-Robo signaling during axon pathfinding at the CNS midline. *J Neurosci* 32, 10035-44.

Smith, N. R. and Prehoda, K. E. (2011). Robust spindle alignment in Drosophila neuroblasts by ultrasensitive activation of pins. *Mol Cell* 43, 540-9.

Speicher, S., Fischer, A., Knoblich, J. and Carmena, A. (2008). The PDZ protein Canoe regulates the asymmetric division of Drosophila neuroblasts and muscle progenitors. *Curr Biol* 18, 831-7.

Ten Hoopen, R., Cepeda-Garcia, C., Fernandez-Arruti, R., Juanes, M. A., Delgehyr, N. and Segal, M. (2012). Mechanism for astral microtubule capture by cortical Bud6p priming spindle polarity in S. cerevisiae. *Curr Biol* 22, 1075-83.

Toyoshima, F., Matsumura, S., Morimoto, H., Mitsushima, M. and Nishida, E. (2007). PtdIns(3,4,5)P3 regulates spindle orientation in adherent cells. *Dev Cell* 13, 796-811.

Toyoshima, F. and Nishida, E. (2007). Integrin-mediated adhesion orients the spindle parallel to the substratum in an EB1- and myosin X-dependent manner. *EMBO J* 26, 1487-98.

Walston, T., Tuskey, C., Edgar, L., Hawkins, N., Ellis, G., Bowerman, B., Wood, W. and Hardin, J. (2004). Multiple Wnt signaling pathways converge to orient the mitotic spindle in early C. elegans embryos. *Dev Cell* 7, 831-41.

Wee, B., Johnston, C. A., Prehoda, K. E. and Doe, C. Q. (2011). Canoe binds RanGTP to promote Pins(TPR)/Mud-mediated spindle orientation. *J Cell Biol* 195, 369-76.

Yu, F., Morin, X., Cai, Y., Yang, X. and Chia, W. (2000). Analysis of partner of inscuteable, a novel player of Drosophila asymmetric divisions, reveals two distinct steps in inscuteable apical localization. *Cell* 100, 399-409.

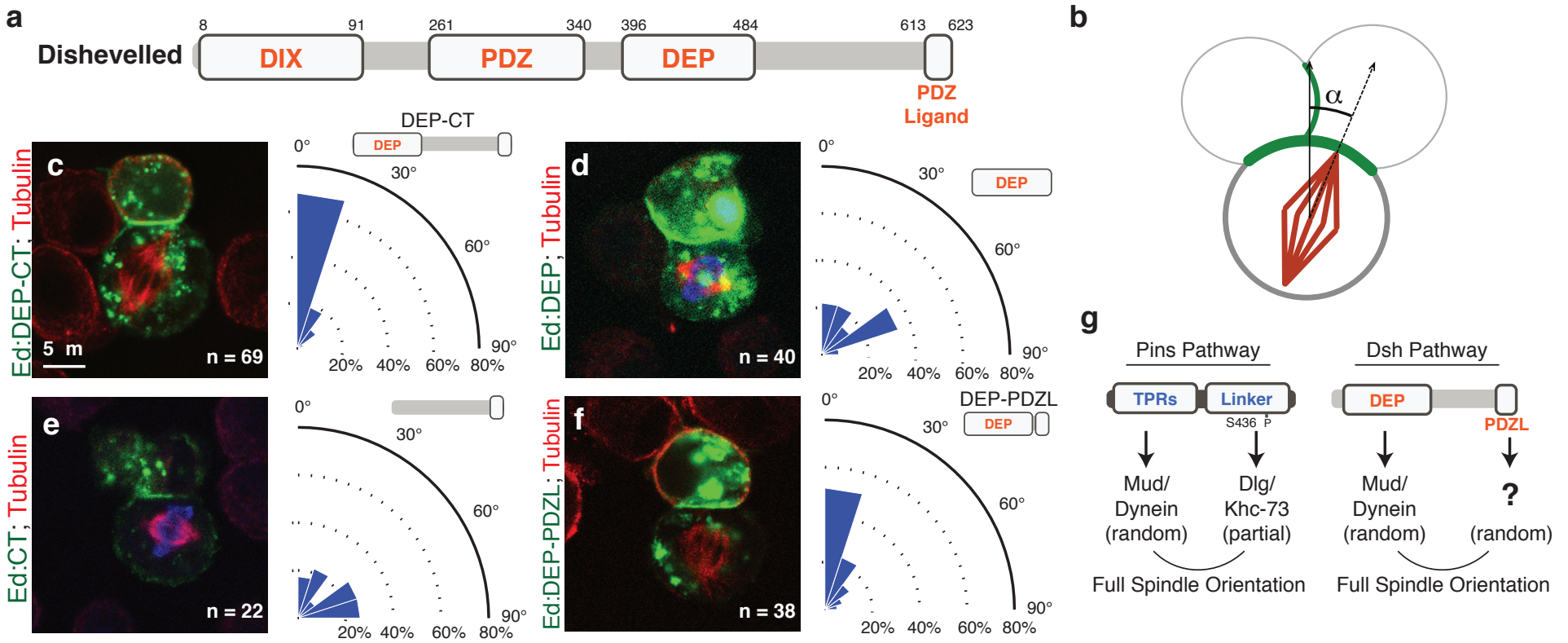

Johnston CA, et al. FIGURE 1

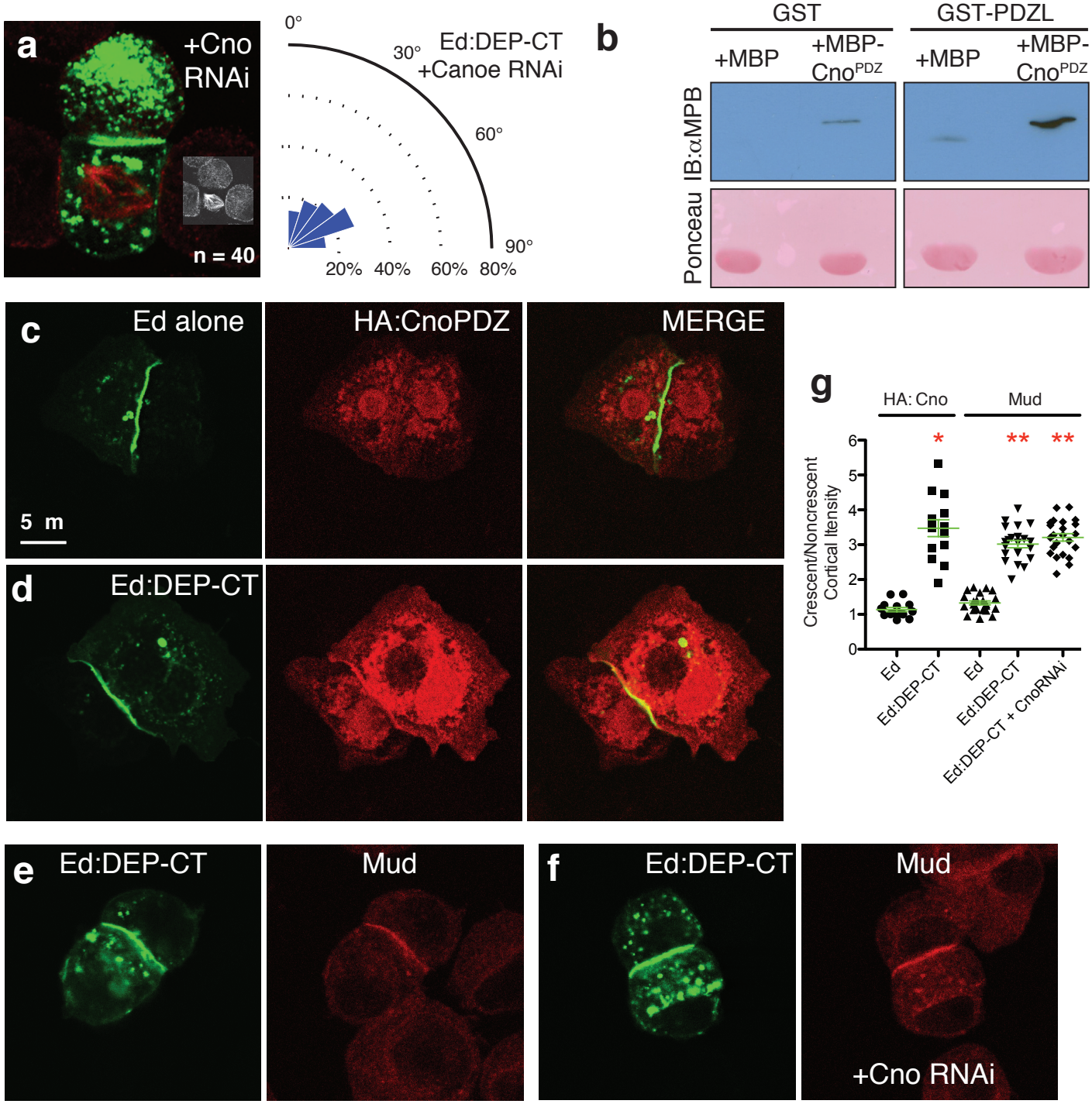

Johnston CA, et al. FIGURE 2

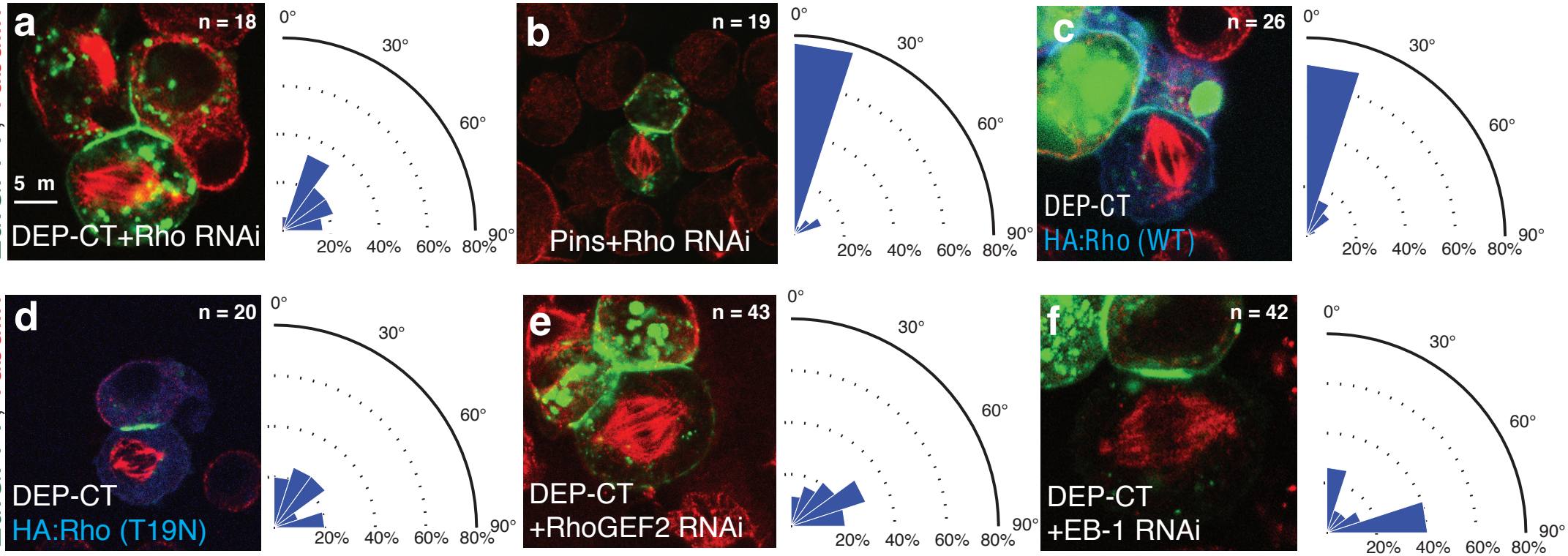

Johnston CA, et al. FIGURE 3

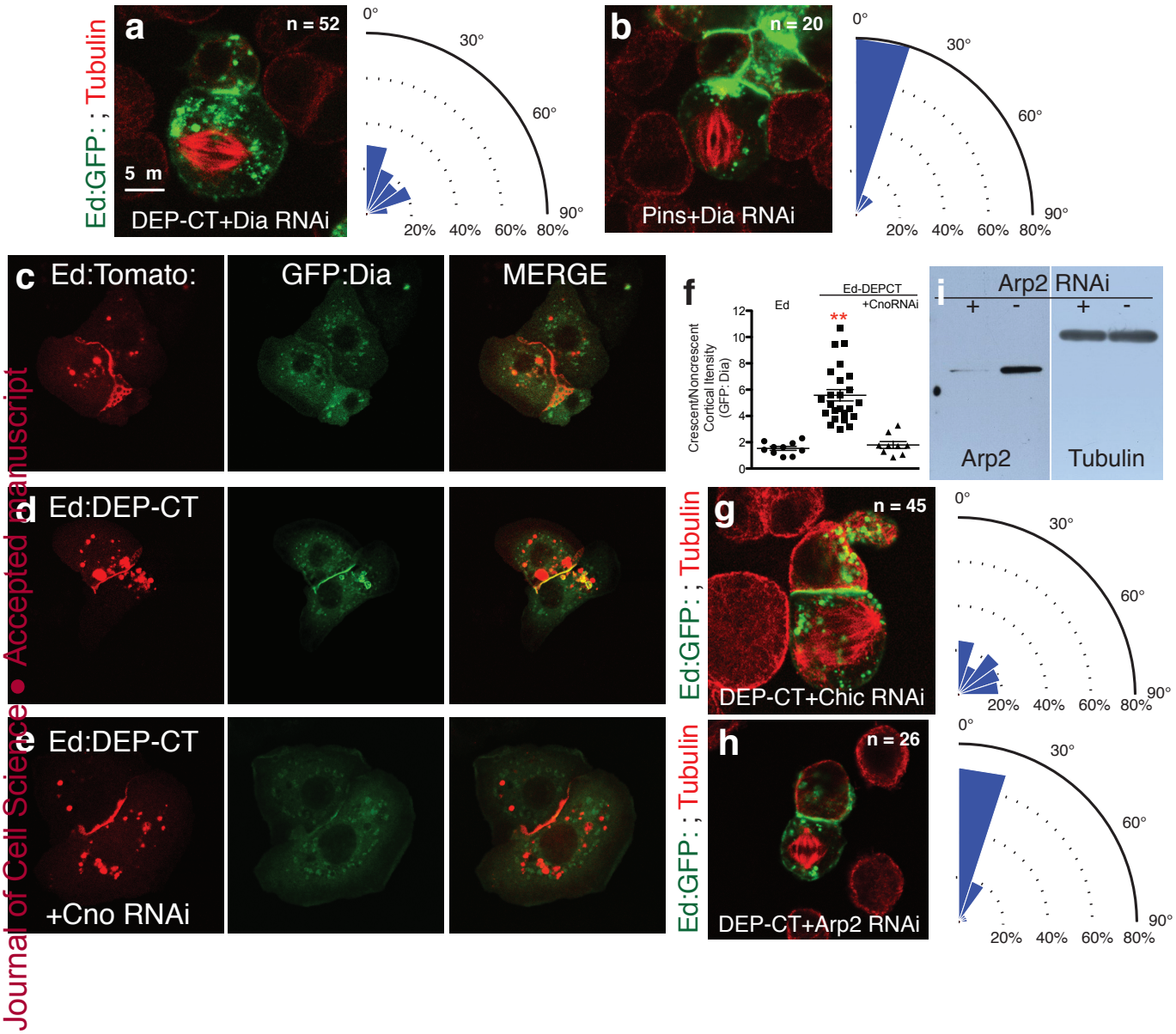

Johnston CA, et al. FIGURE 4

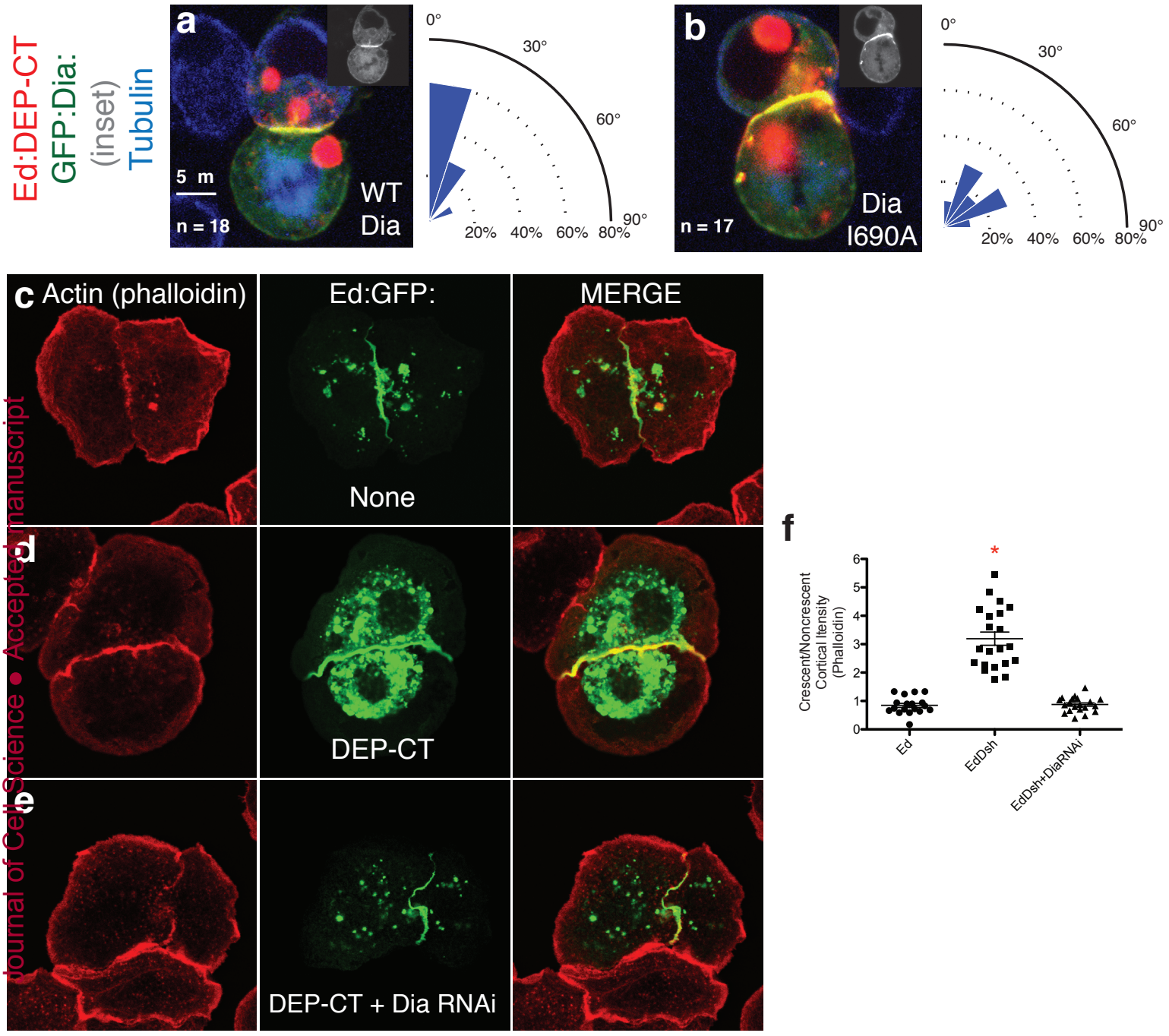

Johnston CA, et al. FIGURE 5

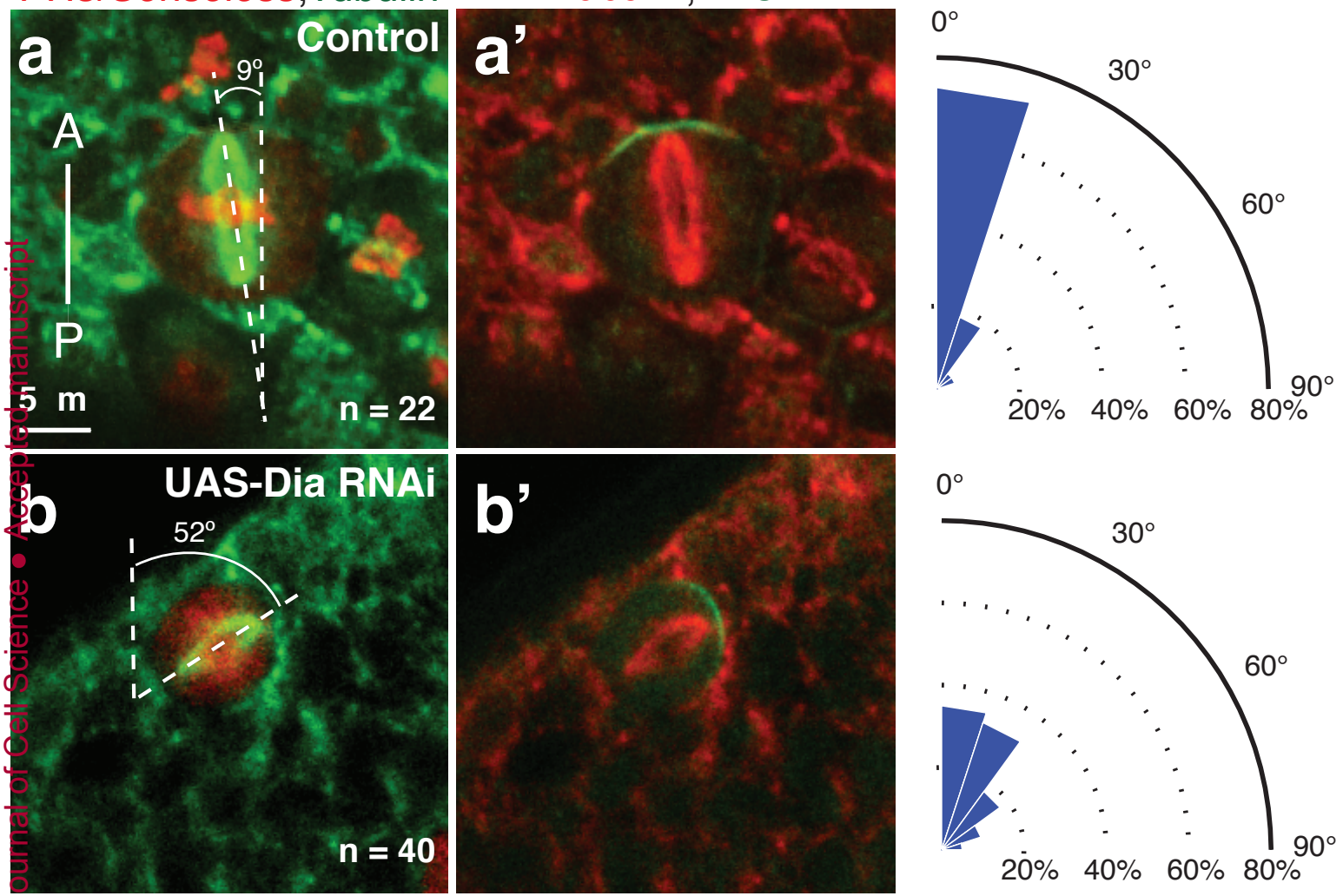

Johnston CA, et al. FIGURE 6

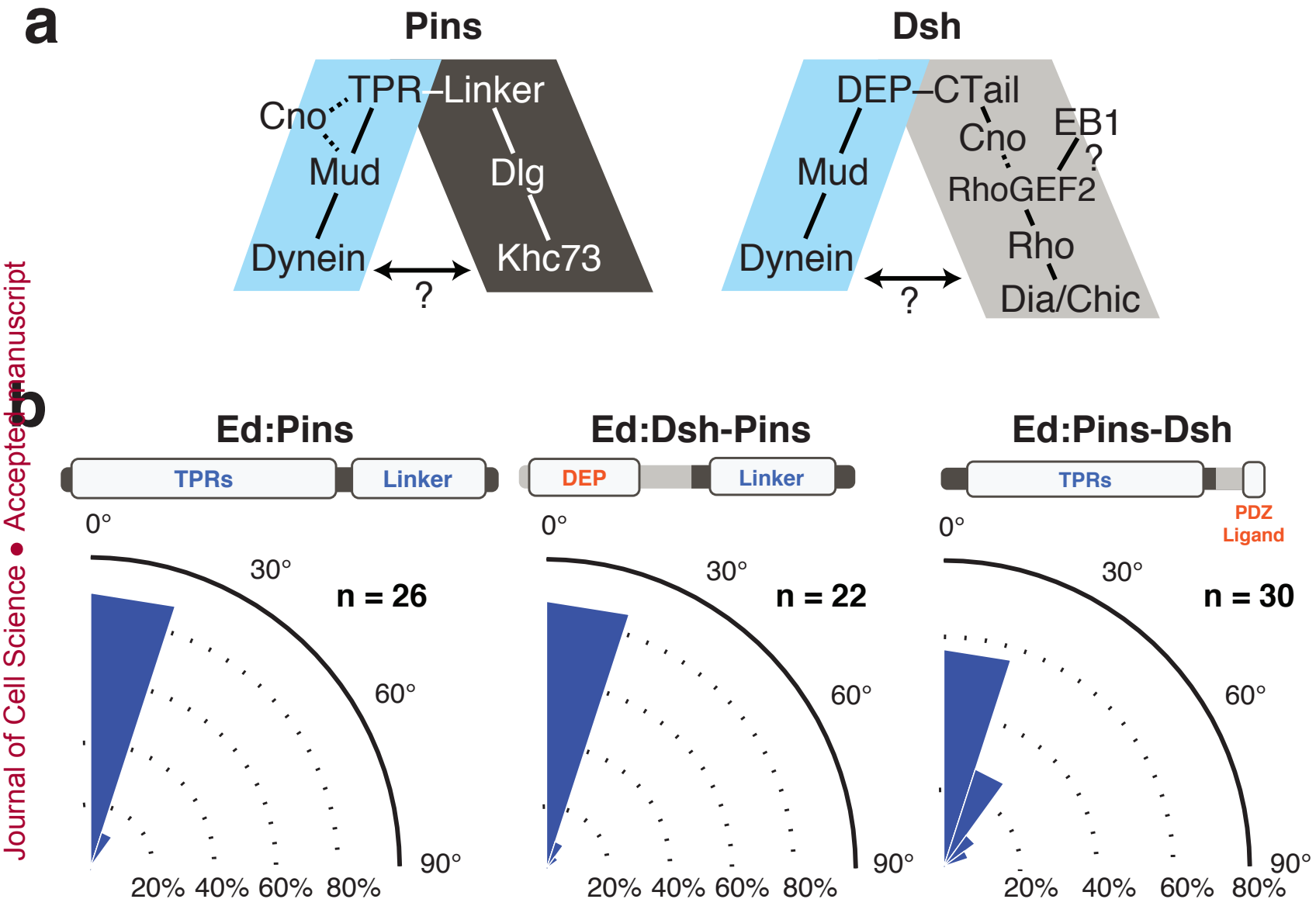

Johnston CA, et al. FIGURE 7